Biosurveillance of Measles using Control Charts: A Case Study using National Capital Region Laboratory Confirmed Measles Counts from January 2009 to January 2014

Lorraine Christelle B. Angkico, Priscilla A. Diaz, Robert Neil F. Leong, and Frumencio F. Co
De La Salle University

This paper aims to explore early outbreak detection methods for measles. Two methods adapted from statistical process control were modified and used to fit biosurveillance, namely Shewhart and Exponentially Weighted Moving Average (EWMA) charts. Seven variations of such control charts are proposed: two under Shewhart chart (normal-based and zero-inflated Poisson (ZIP)-based) and five under EWMA charts (λs of 0.05, 0.10, 0.15, 0.20, and 0.25). To study the proposed charts, daily counts of laboratory confirmed cases of measles in the National Capital Region from 2009 until 2014 were utilized to characterize both the disease background and outbreak equations. During this time span, three measles outbreaks have transpired. The proposed charts, set at average time between false signals (ATFSs) of both one and two months, were evaluated and compared using performance metrics such as conditional expected delay (CED), proportion of true signals (PTS), proportions of detections in an outbreak (PDO), and probability of successful detection(PSD), computed from 500 sets of simulated data. It was found that ZIP-based Shewhart and EWMA with a λ of 0.05 work best for ATFSs of one and two months, respectively. Health-governing bodies may seek to explore the possible utilization of these charts to improve measles surveillance.

Keywords: control charts, measles, early event detection, biosurveillance

1. Introduction

One of the most dreaded communicable diseases is measles. Comparable with influenza and tuberculosis, death caused by this disease reach up to millions worldwide (Brauer and Chavez, 2011). Measles is an airborne disease, meaning that it is transmitted through air. It is considered to be highly contagious, as a person without immunity has a 90% chance of acquiring the disease upon contact with someone infected. Some of measles' early signs and symptoms are fever, runny nose, cough, and rashes all over the body. It is often confused with other diseases that cause rashes like *roseola* and *rubella* or German measles.

If measles is neglected, complications might occur. For pregnant women, it can cause early labor or worse, miscarriage. For children who have acquired the said disease, there is a 10% chance of acquiring ear infection and 20% chance of developing pneumonia. An infected person has a 0.1–0.2% probability of having *encephalitis* or dying (Occucare International, 2012; CDC, 2013).

Even though measles is not considered alarming in the Western hemisphere, the same cannot be said in the Philippines (Brauer and Chavez, 2001; Santos, 2013). In this country, measles is a serious problem, wherein the ones who suffer most are children. In 2011, the recorded number of infected people was over 2,000 nationwide during only the first three months. This figure includes five deaths. During the same time span, the Department of Health (DOH) was also able to identify that National Capital Region (NCR) had the highest number of cases (311) among the country's 17 regions (Aragones, 2011).

Last December 11, 2013, the DOH reported that the cases of measles in Metro Manila multiplied seven times as the year before. The number of cases from January 1 to December 10, 2013 reached 179 including two deaths (RSJ, GMA News, 2013).This most recent epidemic is not only taking its toll in NCR, but also in several other places in the country such as the Cordillera Administrative Region (CAR) and Western Visayas. In CAR, the number of patients was reported to have increased from 30 the past year to 77. Kalibo, Aklan was reported to have been declared in a state of calamity because of a certain measles outbreak (Agreda, 2013; Carcamo, 2013). Due to these occurrences, actions must be done to prevent or, at the very least, to contain the spread of such disease. One possible solution is through improved biosurveillance.

Biosurveillance is a concept that was developed and introduced to the scientific community just two decades ago. According to Dr. M. Wagner, director of Real-Time Outbreak and Disease Surveillance Laboratory, University of Pittsburgh, "biosurveillance is a process which detects and characterizes outbreaks of diseases in people, plants, or animals" (Wagner, 2006). One of its main activities is *epidemiological surveillance*. Epidemiological surveillance is defined in Homeland Security Presidential Directive 21 as "the process of actively gathering and analyzing data related to human health and disease in a population

in order to obtain early warning of human health events, rapid characterization of human disease events, and overall situational awareness of disease activity in the human population" (HSPD-21, 2009).

The objective of this study is to provide biosurveillance, particularly monitoring methods that could efficiently detect measles outbreaks. From this problem derives a key goal that this paper intends to achieve: identify the best monitoring process with the use of different monitoring performance metrics.

Through biosurveillance this study wishes to monitor measles activity in the context of the number of recorded cases over the NCR during the period January 2009 to January 2014. Moreover, it aims to detect outbreaks as early as possible for immediate intervention by the concerned authority. In doing so, less people could get infected; hence, less cost will be incurred. The results of this research may assist the DOH and other health organizations in performing studies related to measles surveillance.

2. Conceptual Framework

2.1. Biosurveillance vs Statistical Process Control

Statistical process control (SPC) and biosurveillance are very similar processes due to their common objectives. SPC's main objective is early detection of unwanted shifts of nonconforming units in a manufacturing process and their possible causes to bring back the process in its original state(Montgomery, 2009). On the other hand, biosurveillance systems have two main objectives: (1) to provide the public with *situational awareness* (SA);and (2) the timely monitoring of an outbreak through enhanced *early event detection* (EED) or the ability to detect a crisis in relation with public health as quickly as possible (Fricker, 2013). This paper aims to focus more on EED.

However, they also have notable differences, some of which are as follows: (1) in SPC, when a process goes out of control, it stays out of control while in biosurveillance, an outbreak is transient or will eventually die down; (2) SPC charts utilize upper and lower control limits to detect shifts, whereas biosurveillance only uses the upper control limit since it is only interested with increases in disease occurrences; and (3) observations in SPC are independent while the observations in biosurveillance are usually autocorrelated. The reason for this is because SPC involves sampling in which the observations are selected far apart enough from each other to make them independent; while biosurveillance utilizes all existing data collected in real-time which brings about autocorrelation. Most of the methods in biosurveillance were adapted from traditional SPC. However, due to their differences, such methods must first be modified to suit the objectives of EED. The methods used for SPC are called control charts while in biosurveillance they are referred to as detection or EED methods (Fricker, 2013). However, in this paper, the two terms may be used interchangeably.

2.2. Early event detection methods

Two EED methods were explored and modified for this study, namely Shewhart and Exponentially Weighted Moving Average (EWMA) charts, both of which are traditional SPC control charts.

2.2.1. Shewhart

The Shewhart detection method is one of the most commonly used SPC procedures. For data possessing normal distribution, it involves the standardization of the sample mean as the Shewhart statistic (S_t), compared with some threshold h>0 for which the process would signal once the statistic exceeds its value. In symbols,

$$S_t = \left| \frac{\overline{Y} - \hat{\mu}_0}{\hat{\sigma}_{\overline{Y}}} \right|. \tag{1}$$

However, since biosurveillance does not involve sampling, the individual observations are standardized using the statistics from the non-outbreak observations. Equation (1) shall now be modified as

$$S_t = \left| \frac{Y_t - \overline{Y}}{\hat{\sigma}_{\overline{Y}}} \right|.$$

This equation will produce a signal once the Shewhart statistic S_t results to a value greater than or equal to the preassigned number h (Fricker, 2013).

Another modification is made for zero-inflated Poisson (ZIP) distributed data. While ZIP-based Shewhart charts have a vast literature regarding applications in monitoring manufacturing processes (Xie et al., 2001; Sim and Lim, 2008; Katemee and Mayureesawan, 2012) and healthcare performances (Woodall, et al., 2012), they have never been used in the context of purely temporal biosurveillance before. Hence in this context, the ZIP-based Shewhart chart threshold value is modified, which in this case is computed as

$$h = \beta + c\sqrt{\beta},$$

for some constant c and

$$\beta = \overline{y}^{+}\left(1 - e^{-\beta}\right),$$

where $\overline{y}^{+}$ is the mean number of all counts greater than zero (Katemee and Mayureesawan, 2012).

2.2.2. EWMA

Another commonly used EED method is EWMA. It uses the weighted averages of past observations. In this paper, EWMA values are reset after every signal (Borror, et al.,1998). The algorithm applied here is composed of moving averages and weights that are assigned to the current and previous observations. The more distant an observation is from the present, the more exponentially decreasing the given weight (Wong and Moore, 2006). The EWMA statistic was introduced as

$$Z_t = \lambda Y_t + (1-\lambda)Z_{t-1} \tag{2}$$

and

$$Z_0 = \mu_0,$$

with variance

$$Var(Z_t) = \frac{\lambda}{2-\lambda}\left[1-(1-\lambda)^{2t}\right]\mu_0 \approx \frac{\lambda\mu_0}{2-\lambda} = Var(Z_\infty),$$

where Y_t is the observed value at time t, λ is the weight assigned to the observation which has a range of [0,1] but is more desired to be within [0.05,0.25], and μ_0 is the process mean of all observations given that it is in-control (Montgomery, 2009; Borror, Champ, and Rigdon, 1998; Shu, Jiang, and Wu, 2012). As with any EED statistic, equation (2) must be modified into

$$Z_t = \max\left[\mu_0, \lambda Y_t + (1-\lambda)Z_{t-1}\right].$$

A signal is observed at time t when Z_t is greater than the threshold h defined as

$$h = \mu_0 + L\hat{\sigma}\sqrt{Var(Z_t)}.$$

One of the properties of EWMA is that for a non-normal data, it can be robust (Borror, Montgomery, and Runger, 1999). Thus, it is not restricted to certain distributions. In addition, it also works well with Poisson distributed data (Fricker, 2013; Shu, et al., 2012; Woodall, et al., 2012).

2.3. Performance metrics

The metrics to be used to assess the EED methods are as follows:

(a) Average time between false signals (ATFS),
(b) Conditional expected delay (CED), and
(c) Probability of successful detection (PSD).

In addition to these metrics which are commonly used in literature (Fricker, 2013; Borror, et al., 1998; Shu, Jiang, and Wu, 2012; He, Li, and He, 2014), the following are also proposed:

(d) Proportion of true signals (PTS), and
(e) Proportion of detections in an outbreak (PDO).

The ATFS, as its name suggests, is the expected number of time periods before the system signals given the absence of an outbreak. In comparison to the usual statistical tests, it is similar to the specificity metric. On another note, ATFS is the counterpart of ARL_0 in SPC. ARL_0 is the average run length given that the process is in-control. ATFS is computed as

$$ATFS = E\,(t^{**} - t^{*} \mid \tau_s = \infty), \tag{3}$$

where t^* is the time of the first signal in the method, t^{**} is the time of the next signal, and τ_s is the time period when the outbreak started (Woodall, 2006). The expression $\tau_s = \infty$ means that no outbreak will occur.

The CED, similar with ARL_1 in SPC, is the time lag before the method first signals during an outbreak. ARL_1 is the average run length given that the process is out-of-control. CED is computed as

$$CED = E\,(t^{*} - \tau_s \mid \tau_s \leq t^{*} \leq \tau_l), \tag{4}$$

where t^* and τ_s are defined similarly as in equation (3), and τ_l is the time period when the outbreak ends. However, a notable difference between CED and ARL_1 is that ARL_1 is clearly finite while CED may be ∞ (i.e., the outbreak is never detected).

The PSD is the probability that the method signals within the significant portion of an outbreak. In this paper, a signal is considered significant for as long as the number of cases is still increasing. It is given by

$$PSD = \mathrm{P}\,(\tau_s \leq t^{*} \leq \tau_r), \tag{5}$$

where t^* and τ_s are defined as in equations (3) and (4), and τ_r is the last period in which the outbreak detection is still considered significant.

Another metric considered in this study is PTS, which is the probability that the generated signals are within an outbreak period. This metric is similar to the positive predictive value. It is given by

$$PTS = P\,(\tau_s \leq \tau_i \leq \tau_l \,|\, Y_{\tau_i} > h), \tag{6}$$

where τ_s and τ_l are defined similarly as in equations (3) and (4), Y_{τ_i} is the statistic from any of the EED methods observed at time τ_i, and h is its corresponding threshold.

Lastly, the PDO refers to the probability that a signal is generated within an outbreak period. This metric is similar to sensitivity. Mathematically, it can be expressed as

$$PDO = P\,(Y_{\tau_i} > h \mid \tau_s \leq \tau_i \leq \tau_l), \tag{7}$$

where τ_s, τ_l,τ_i Y_{τ_i}, and h are defined as in equation (6) (Fricker, 2013).

3. Methodology

3.1. Data

The data used in this study, obtained from the Regional Epidemiology and Surveillance Unit (RESU), are the daily count of laboratory confirmed measles cases in NCR from January 2009 to January 2014 (1,842 days). A time series graph of the data is shown in Figure 1. In this particular graph, three significant shifts from the mean are observed. After confirmation from news reports, these shifts are identified as outbreaks (Aragones, 2011; RSJ, GMA News, 2013; Agreda, 2013). The outbreak periods identified are the following:

Outbreak 1: January 1, 2010 to April 30, 2010 (120 days),
Outbreak 2: January 1, 2011 to May 31, 2011 (151 days), and
Outbreak 3: October 1, 2013 to January 16, 2014 (108 days).

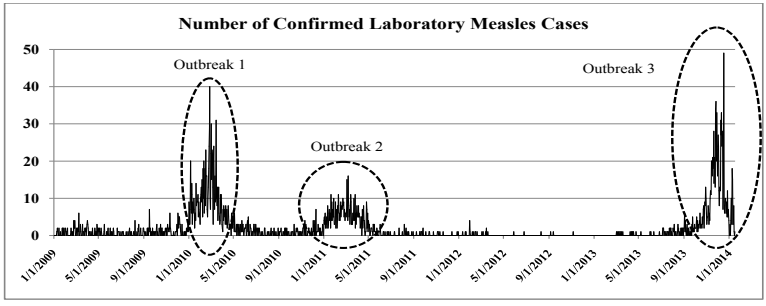

Figure 1. Number of Confirmed Laboratory Measles Cases in NCR from January 1, 2009 to January 16, 2014

3.2. Simulation

To assess the appropriateness of the proposed EED methods, simulations were performed and studied using the R software. To perform simulations, periods classified as outbreaks were removed to establish baseline data. Then, the background disease distribution was identified, which in this case followed a ZIP distribution. The density function of ZIP is as follows:

$$f\left(Y_i = y_i; \pi, \lambda\right) = \begin{cases} \pi + \left(1-\pi\right)e^{-\theta}, y_i = 0 \\ \left(1-\pi\right)\dfrac{\theta^x e^{-\theta}}{y!}, y_i = 1,2,... \end{cases},$$

where Y is discrete, which in this paper is the number of daily measles cases; π is the probability of additional zeros; and θ is the expected i^{th} number of occurrences. ZIP distribution has found its first applications in the detection of manufacturing defects, where the parameter π is the probability of observing a perfect zero-defect state and θ is the Poisson intensity of observing defects when the process state is misaligned (Lambert, 1992). More recently, aside from applications in manufacturing processes, the distribution has now been explored for possible applications in modelling healthcare performances and surveillance (Woodall, Adams, and Benneyan, 2012).

The method of moments estimators of the parameters of a ZIP distribution are

$$\hat{\theta}_{MOM} = \frac{s^2 - \overline{x} + \overline{x}^2}{\overline{x}}$$

and

$$\hat{\pi}_{MOM} = \frac{s^2 - \overline{x}}{s^2 - \overline{x} + \overline{x}^2},$$

where $\overline{x}$ and s^2 are the sample mean and variance, respectively (He, Li, and He, 2014).A χ^2-goodness-of-fit test validated the assumption that the baseline data followed a ZIP distribution with estimated parameters $\hat{\pi}_{MOM}$ = 0.6146 and $\hat{\theta}_{MOM}$ = 1.1844. Simulations were performed to generate 500 data sets replicating the performance of the baseline data.

3.3. Pre-setting of ATFS

To allow comparability of the other four metrics discussed in Section 2.3., it would be necessary to preset ATFS since it is practical to determine how far apart investigations of outbreaks must be. In this study, presetting of ATFS is

established through the Shewhart method. SPC's Shewhart method for normally distributed data has a standardized threshold of 3, while in biosurveillance, it has a standardized threshold of 2 (Woodall, Adams, and Benneyan, 2012). Using these, the simulated baseline data generated ATFSs with a mean of 25 (h = 2) and 70 (h = 3) days, or approximately one and two months, respectively. Appropriate thresholds were then determined for the other Shewhart-type based on a ZIP distribution and for EWMA with five different values of λ to achieve the desired ATFSs.

3.4. Outbreak injection

The identified outbreaks were modelled in order to inject them in the simulated data. The outbreaks can be categorized into patterns or shapes that they resemble, namely: triangular, ramp, and spike. However, modifications and combinations of these patterns were done to capture the outbreaks' behavior. It is assumed that the outbreaks are additive and deterministic in the background series. The general equation for a triangular outbreak pattern is as follows:

$$o_t = \begin{cases} \dfrac{2M\left(t-\tau+1\right)}{D+1}, \text{outbreak is increasing} \\ \dfrac{2M\left(D+\tau-1\right)}{D+1}, \text{outbreak is increasing} \\ 0 \qquad\qquad , \text{otherwise} \end{cases},$$

where M is the maximum magnitude of the outbreak, D is the duration of the outbreak, and τ is its starting time. The value of τ is usually set to 1, so that t would range from 1 to D (Fricker, 2013). On the other hand, the general equation for a ramp and spike outbreak pattern is

$$o_t = \begin{cases} M, \text{ outbreak is existing} \\ 0, \text{ otherwise} \end{cases},$$

where M will still be the maximum magnitude for a spike pattern and the mean magnitude of the outbreak for a ramp pattern.

The first outbreak showed exponential growth-and-decay patterns (see Figure 2).The outbreak equation injected is given by

$$o_{1_t} = \begin{cases} \exp\left(\dfrac{79.08t}{121}\right) & , 1 \le t \le 60 \\ \exp\left(\dfrac{79.08(121-t)}{121}\right) & , 61 \le t \le 120 \\ 0 & , \text{otherwise} \end{cases}.$$

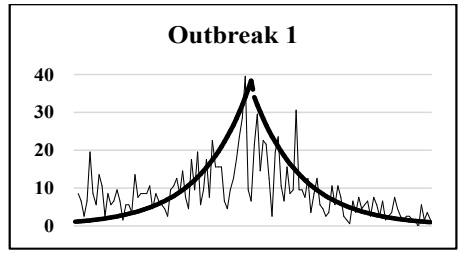

Figure 2. Actual (straight line) vs. Modelled (dashed line) Counts for the First Outbreak

The pattern of the second outbreak showed a combination of triangle and ramp patterns (see Figure 3). The outbreak equation injected is given by

$$o_{2_t} = \begin{cases} \dfrac{31.08t}{152} & ,1 \le t \le 22 \\ 5.81 & ,23 \le t \le 61 \\ \dfrac{31.08(t-56)}{152} & ,62 \le t \le 68 \\ \dfrac{31.08(80-t)}{152} & ,69 \le t \le 78 \\ 4.15 & ,79 \le t \le 119 \\ \dfrac{7.08(152-t)}{152} & ,120 \le t \le 15 \\ 0 & ,\text{otherwise} \end{cases} .$$

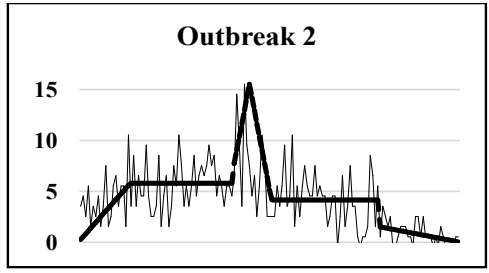

Figure 3. Actual (straight line) vs. Modelled (dashed line) Counts for the Second Outbreak

The pattern of the third outbreak showed a combination of two exponential growths and linear decays (see Figure 4).The outbreak equation injected is given by

$$o_{3_t} = \begin{cases} \exp\left(\dfrac{71.08(t-45)}{78}\right) & ,1 \le t \le 54 \\ \dfrac{71.08(123-t)}{78} & ,55 \le t \le 92 \\ \exp\left(\dfrac{35.08(t-15)}{124}\right) & ,93 \le t \le 100 \\ \exp\left(\dfrac{35.08(139-t)}{124}\right) & ,101 \le t \le 108 \\ 0 & ,\text{otherwise} \end{cases} .$$

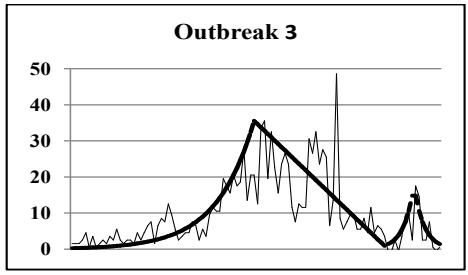

Figure 4. Actual (straight line) vs. Modelled (dashed line) Counts for the Third Outbreak

Seven EED methods were studied through simulations, two were Shewhart-based: one based on a normal distribution and another based on a ZIP distribution; and five were EWMA charts using different values of λ: 0.05, 0.10, 0.15, 0.20, and 0.25. These EED methods were compared empirically using summary statistics of the four other performance metrics (CED, PSD, PTS, and PDO) taken over the 500 simulations. Similar procedure was also done with the actual data.

4. Results and Discussion

Four kinds of outbreak simulations were made in each data set; three of which considered each outbreak one at a time and another with all outbreaks injected all at once. This is to see if there is a difference when the outbreaks are injected individually or simultaneously. All the results for CED, PTS, and PDO are shown in Tables 1, 2 and 3, respectively. Moreover, visualizations of distributions of the same metrics are provided in Figure 5.

Comparing the Shewhart methods at both ATFSs, as shown in Table 1, lower CED values were observed with the ZIP-based method. That is, it can detect outbreaks faster by a day or two. Regarding PDO and PTS metrics from Tables 2 and 3, values closer to one are more desirable. While the PDO values produced desirable values for both methods, ranging from 0.73 to 0.97, PTS values are

quite low. Particularly, very low values of PTS were observed when outbreaks are injected individually and thresholds were set based on an ATFS of one month (e.g., 0.5737 for normal-based and 0.4425 for ZIP-based Shewhart charts in outbreak 1). CED values, again from Table 1, vary a lot in both Shewhart charts as evidenced by their coefficients of variation (e.g.,53% vs 57% at an ATFS of one month and 40% vs 39% at an ATFS of two months when all outbreaks are injected for normal-based and ZIP-based Shewhart charts, respectively). On the contrary, PTS and PDO values vary slightly with the normal-based being more precise for the former and the ZIP-based for the latter. For instance, PTS and PDO correspondingly yielded coefficients of variation of 2% and 3% for normal-based and 13% and 1% for ZIP-based when all outbreaks are injected with an ATFS of one month. With a focus on determining a timely EED method, CED is given more importance. Hence, ZIP-based Shewhart chart is preferred over the normal-based Shewhart chart as evidenced by a lower mean CED along with a comparable precision. Nevertheless, both PTS and PDO metrics slightly favor that of ZIP-based Shewhart chart.

For EWMA charts, the results for five different values of λ (i.e. 0.05, 0.10, 0.15, 0.20, and 0.25) are obtained. From Figure 6, it can be deduced that CED and PTS yielded similar patterns as a function of λ. On the other hand, PDO yielded an inverted pattern of the other two.

Referring to Table 1, $\lambda = 0.10$ and $\lambda = 0.05$ provided the lowest values of CED for an ATFS of one and two months, respectively. However, from Tables 2 and 3, the best λs for PTS and PDO at both ATFSs are 0.15 and 0.20, respectively. Comparing the variations of the same metrics, the CVs for CED ranged from 22% to 90% signifying high variation with $\lambda = 0.15$ being the most precise(i.e. 22% is the lowest CV among the λ's for an ATFS of two months when all outbreaks are injected). In view of PTS and PDO, both registered low CVs ranging from 1% to 15% and 1% to 14%, respectively.

Table 1. Means and Coefficients of Variation (CVs) Given by the 500 Simulations for the Conditional Expected Delay

CED		Outbreak 1				Outbreak 2			
		mean		CV		mean		CV	
		1 mo	2 mos	1 mo	2 mos	1 mo	2 mos	1 mo	2 mos
Shewhart	Normal	4.1780	7.5720	79%	67%	3.0200	4.7740	156%	52%
	ZIP	2.6980	6.1960	110%	81%	2.5520	4.4560	64%	54%
EWMA	0.05	2.5680	3.3640	56%	48%	2.7880	3.3280	49%	42%
	0.10	2.2440	4.1940	59%	69%	2.9060	3.8700	43%	35%
	0.15	3.3440	5.3160	49%	38%	3.2460	4.2660	40%	30%
	0.20	2.2900	4.4580	60%	67%	3.1120	3.8460	63%	34%
	0.25	2.8360	4.3267	56%	53%	2.8080	3.6500	50%	39%

CED		Outbreak 3				All Outbreaks			
		Mean		CV		mean		CV	
		1 mo	2 mos	1 mo	2 mos	1 mo	2 mos	1 mo	2 mos
Shewhart	Normal	6.8080	13.7500	91%	67%	4.6687	8.6987	53%	40%
	ZIP	6.1800	12.8700	91%	61%	3.8100	7.8407	57%	39%
EWMA	0.05	7.9860	9.7780	81%	45%	4.4473	5.4900	51%	30%
	0.10	7.2980	10.5320	90%	44%	4.0493	6.3253	37%	33%
	0.15	10.4440	13.8740	67%	35%	5.6780	7.8187	43%	22%
	0.20	7.5480	11.2480	65%	62%	4.4093	6.4640	42%	34%
	0.25	8.6060	11.9560	82%	46%	4.7500	6.6757	43%	31%

Table 2. Means and Coefficients of Variation (CVs) Given by the 500 Simulations for the Proportion of True Signals

PTS		Outbreak 1				Outbreak 2			
		mean		CV		mean		CV	
		1 mo	2 mos	1 mo	2 mos	1 mo	2 mos	1 mo	2 mos
Shewhart	Normal	0.5737	0.7766	11%	10%	0.6550	0.8481	4%	7%
	ZIP	0.4425	0.6709	29%	21%	0.5288	0.7601	24%	15%
EWMA	0.05	0.6665	0.7555	9%	4%	0.7469	0.8185	3%	3%
	0.10	0.5915	0.7744	5%	4%	0.6840	0.8304	4%	3%
	0.15	0.8219	0.8207	9%	12%	0.8560	0.8722	8%	8%
	0.20	0.5937	0.7670	5%	4%	0.6796	0.8398	5%	3%
	0.25	0.7160	0.7934	14%	5%	0.7760	0.8520	9%	3%

PTS		Outbreak 3				All Outbreaks			
		Mean		CV		mean		CV	
		1 mo	2 mos	1 mo	2 mos	1 mo	2 mos	1 mo	2 mos
Shewhart	Normal	0.5185	0.7110	6%	11%	0.8321	0.8320	2%	4%
	ZIP	0.3999	0.6405	31%	23%	0.7371	0.8838	13%	7%
EWMA	0.05	0.6182	0.7323	5%	5%	0.8825	0.9234	2%	1%
	0.10	0.5341	0.7480	14%	5%	0.8493	0.9294	2%	1%
	0.15	0.8021	0.7963	10%	13%	0.9454	0.9444	3%	3%
	0.20	0.5502	0.7393	5%	5%	0.8501	0.9299	2%	1%
	0.25	0.6692	0.7675	15%	5%	0.9034	0.9376	5%	1%

Table 3. Means and Coefficients of Variation (CVs) Given by the 500 Simulations for the Proportion of Detections in an Outbreak

PDO		Outbreak 1				Outbreak 2			
		mean		CV		mean		CV	
		1 mo	2 mos	1 mo	2 mos	1 mo	2 mos	1 mo	2 mos
Shewhart	Normal	0.8910	0.7313	8%	3%	0.8684	0.9328	11%	1%
	ZIP	0.8521	0.7391	2%	3%	0.9643	0.9490	1%	2%
EWMA	0.05	0.7682	0.7071	1%	1%	0.9312	0.8036	1%	1%
	0.10	0.8018	0.7194	2%	1%	0.9468	0.8090	1%	1%
	0.15	0.7096	0.7086	5%	6%	0.8145	0.8515	5%	9%
	0.20	0.8120	0.7398	2%	2%	0.9503	0.9281	1%	1%
	0.25	0.8044	0.7437	2%	2%	0.9387	0.8714	3%	7%

PDO		Outbreak 3				All Outbreaks			
		Mean		CV		mean		CV	
		1 mo	2 mos	1 mo	2 mos	1 mo	2 mos	1 mo	2 mos
Shewhart	Normal	0.8159	0.7064	5%	3%	0.8436	0.7974	3%	1%
	ZIP	0.7901	0.7112	2%	2%	0.8740	0.8019	1%	1%
EWMA	0.05	0.7296	0.6960	2%	1%	0.8118	0.7390	3%	1%
	0.10	0.7419	0.7021	14%	2%	0.8439	0.7469	1%	1%
	0.15	0.6935	0.6867	6%	5%	0.7568	0.6978	1%	1%
	0.20	0.7703	0.7281	2%	7%	0.8500	0.8019	1%	1%
	0.25	0.7644	0.7106	2%	2%	0.8409	0.7819	2%	4%

Again with a focus on early detection of outbreaks, CED is given more importance. This would entail looking into whether there are considerable differences among the values of the best λs for PTS and PDO (i.e. 0.15 and 0.20) against the best λs for CED (i.e. 0.05 and 0.10). The differences between these two sets of λs are not substantially large except for PTS at an ATFS of one month when the outbreaks are injected individually (see Table 2), and for CED on both ATFS when only outbreak 3 is injected (see Table 1). To illustrate, the mean PTS value for outbreak 1 at an ATFS of one month for $\lambda = 0.10$ is 0.5915, while for $\lambda = 0.15$ is 0.8219. Such discrepancy can also be seen in outbreaks 2 (0.6840 vs. 0.8560) and 3 (0.5341 vs. 0.8021). On the other hand, the mean CED values for outbreak 3 at an ATFS of one month for $\lambda = 0.10$ is 7.2980, while for $\lambda = 0.15$ is 10.4440. This is also the case at an ATFS of two months (9.7780 for $\lambda = 0.05$ vs. 13.8740 for $\lambda = 0.15$). However, since the differences among other CED values are not considerably large, the recommended λ is 0.15 for an ATFS of one month and 0.05 for two months.

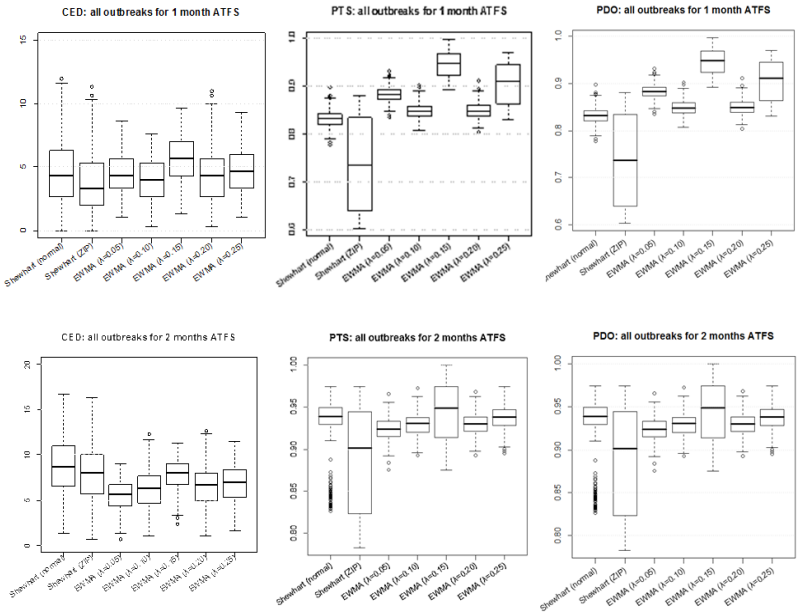

Figure 5. Boxplots of the means for CED, PTS, and PDO when all outbreaks are injected simultaneously at both ATFS

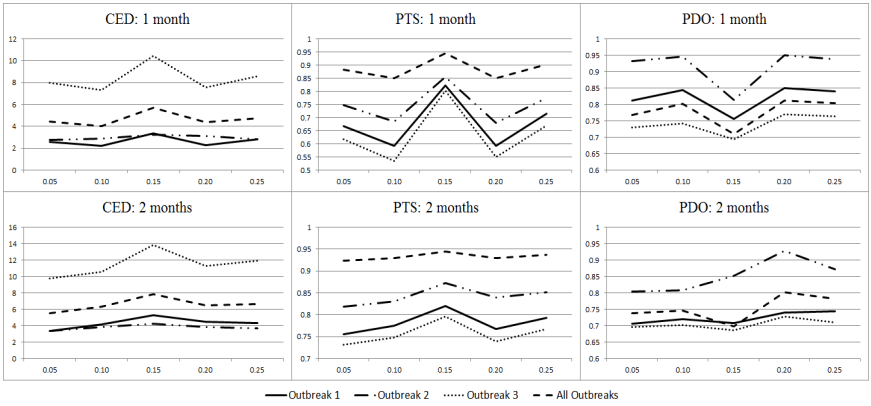

Figure 6. Illustrations of the computed values for CED, PTS, and PDO for different λs in EWMA charts

The last metric that is considered is PSD, which in this paper is defined as

$$PSD = P(\tau_s \le t^* \le \tau_r) = \begin{cases} 1, CED < m \\ 0, otherwise \end{cases},$$

where m is the time when an outbreak is at its peak. The values of m are 60, 68, and 54 for outbreaks 1, 2, and 3, respectively. For all seven EED methods, the value of PSD is observed to be one, indicating that all outbreaks are detected successfully.

As mentioned above, the Shewhart method that gave the most desirable results is the ZIP-based method for both ATFSs; while with EWMA, the most preferred λs are 0.15 for an ATFS of one month and 0.05 for two months. Comparing these two methods at an ATFS of one month, the Shewhart method is preferred since it provided more desirable results in terms of CED and PDO. On the other hand, at an ATFS of two months, the EWMA method, specifically with $\lambda = 0.05$, is preferred since it provided better results in terms of CED and PTS.

The same EED methods were evaluated using the same performance metrics as observed with the original data. The values are summarized in Table 4. Of the three metrics, PTS and PDO were observed to be very different from the simulation results. Here, it can be seen that Shewhart charts outperform EWMA charts. Regarding CED, some EWMA charts performed better than Shewhart charts, particularly at an ATFS of one month. A possible reason for the discrepancy may be attributed to the presence of autocorrelation in the original series. Hence, the power of Shewhart charts must not be discounted in the surveillance of measles.

Table 4. Performance Metrics Observed with the Original Data

All Outbreaks		CED		PTS		PDO	
		1 mo	2 mos	1 mo	2 mos	1 mo	2 mos
Shewhart	Normal	1.0000	1.3333	0.8228	0.4000	0.8206	0.7071
	ZIP	1.0000	1.3333	0.4642	0.4000	0.8206	0.7071
EWMA	0.05	0.6667	3.6667	0.4360	0.2388	0.7546	0.3087
	0.10	1.3333	0.6667	0.5815	0.3788	0.6306	0.4987
	0.15	1.0000	2.3333	0.4171	0.4049	0.4380	0.3483
	0.20	2.0000	1.6667	0.5105	0.3988	0.4485	0.3536
	0.25	1.0000	1.0000	0.4853	0.4028	0.3931	0.3008

5. Conclusion

In this paper, the best control chart monitoring process for measles at ATFS levels of one and two months were identified to be the ZIP-based Shewhart method and $\lambda = 0.05$ from EWMA, respectively. These were obtained by comparing

performance metrics computed from 500 sets of simulated data replicating the background distribution of measles. Both processes provided low values of CED and high values of PTS and PDO. Low CED values pertain to quick detection of outbreaks; therefore, immediate medical intervention may be given. Moreover, high PTS values pertain to fewer false signals; thus, unnecessary investigations will be minimized. With these findings, health-governing bodies may seek to explore the possible utilization of these charts to improve measles surveillance. Particularly, the efficiency of these charts in performing measles surveillance may further be evaluated in comparison with the current system being implemented by DOH, which is based on weekly or monthly averages during the past three to five years +/- two standard deviations (DOH, 2008).

Biosurveillance, being a relatively new science, demands further research for better understanding. This paper contains the simplest forms of biosurveillance techniques and shall serve as a starting point for other studies that emphasize the use and development of EED methods.

6. Recommendation

It is recommended for future researches to explore more methods, particularly modifications of controls charts accounting for autocorrelation. This is to provide a sound surveillance of infectious diseases like measles. One possible solution is to consider non-resetting of the EWMA charts. In doing so, the statistic for a particular time period is affected by the previous time period, hence accounting for some degree of autocorrelation in the original series. Also, more complex simulation models may be considered to dynamically capture both the background and outbreak behaviors. Lastly, more performance metrics can be utilized in order to assess EED methods performances in different perspectives.

ACKNOWLEDGMENT

The authors would like to extend their sincerest gratitude to the Regional Epidemiologyand Surveillance Unit of the Department of Health for providing the necessary data for this research.

REFERENCES

AGREDA, J. M., 2013, Measles cases soar high by 157%. Retrieved from *Sun Star*,http://www.sunstar.com.ph/baguio/local-news/2013/05/24/measles-cases-soar-157-283866, May 24.

ARAGONES, S., 2011, Over 2000 measles cases in Jan-March. Retrieved from *ABS-CBN News*, http://www.abs-cbnnews.com/lifestyle/04/05/11/over-2000-measles-cases-jan-march, April 5.

BORROR, C.M., CHAMP, C.W., & RIGDON, S.E., 1998, Poisson EWMA control charts, *Journal of Quality Technology* 30 (4): 352-361.

BORROR, C.M., MONTGOMERY, D.C., and RUNGER, G.C., 1999, Robustness of the EWMA control chart to non-normality *Journal of Quality Technology* 31(3): 309-316.

BRAUER, F. and CHAVEZ, C.C., 2001, Basic ideas of mathematical epidemiology. In *Mathematical Models in Population Biology and Epidemiology*, New York: Springer-Verlag New York Inc., pp. 275-276.

CARCAMO, D., 2013, Kalibo under state of calamity over measles outbreak. Retrieved from *The Philippine Star*: http://www.philstar.com/nation/2013/09/05/1175381/kalibo-under-state-calamity-over-measles-outbreak, September 5.

CDC, 2013, Overview of measles. Retrieved from Center for Disease Control and Prevention: http://www.cdc.gov/measles/about/overview.html

DOH, 2008, Manual of procedures for the Philippine Integrated Disease Surveillance and Response (PIDSR). N. T. Catindig, M. O. Niñal, and V. G. Roque, Jr. (Eds.).

FRICKER, R.D., 2013, *Introduction to Statistical Methods for Biosurveillance: With an Emphasis on Syndromic Surveillance*, New York: Cambridge University Press.

HE, S., LI, S., and HE, Z., 2014, A combination of CUSUM charts for monitoring a zero-inflated Poisson process. *Communications in Statistics - Simulation and Computation* 43(10): 2482-2497.

HSPD-21: PUBLIC HEALTH AND MEDICAL PREPAREDNESS, 2009, Retrieved from US Government: http://www.fast.org/irp/offdocs/nspd/hspd-21.htm, September 29.

KATEMEE, N., and MAYUREESAWAN, T., 2012, Control charts for zero-inflated Poisson models, *Applied Mathematics Sciences*, 6(52): 2791-2803.

LAMBERT, D., 1992, Zero-inflated Poisson regression, with an application to defects in manufacturing. *Technometrics* 34(1): 1-14.

MONTGOMERY, D.C., 2009, *Introduction to Statistical Quality Control* (6th ed.), New Jersey, United States of America: John Wiley and Sons, Inc.

OCCUCARE INTERNATIONAL, 2012, Risk of infection East and Southwest Asia. Retrieved from Occupational Health Service: http://occucareinternational.com/blog/wp-content/uploads /2012/05/East-and-southeast-asia.pdf.

RSJ, GMA NEWS, 2013, DOH issues measles alert in NCR as cases rise. Retrieved from GMA Network News: http://www.gmanetwork.com/news/story /339346/news/metromanila/doh-issues-measles-alert-in-ncr-as-cases-rise, December 11.

SANTOS, T. G., 2013, Measles cases up in Metro, says DOH. Retrieved from *The Philippine Daily Inquirer*: http://newsinfo.inquirer.net/544665/measles-cases-up-in-metro-says-doh, December 11.

SHU, L., JIANG, W., & WU, Z., 2012. Exponentially weighted moving average control charts for monitoring increases in Poisson rate, *IIE Transactions* 44(9): 711-723.

SIM, C. H. and LIM, M. H., 2008, Attribute charts for zero-inflated Poisson processes. *Journal of Communications in Statistics – Simulation and Computation* 37(7): 1440-1452.

WAGNER, M.M., 2006, Introduction. In M.M. Wagner, A.W. Moore, and R.M. Aryel (Eds.), *Handbook of Biosurveillance*, Burlington: Elsevier Academic Press, pp.3-12.

WONG, W.K. and MOORE, A.W., 2006, Classical time-series method for biosurveillance. In M.M. Wagner, A.W. Moore, and R.M. Aryel (Eds.), *Handbook of Biosurveillance*. Burlington: Elsevier Academic Press, pp.217-234.

WOODALL, W.H., 2006. The use of control charts in health-care and public-health surveillance, *Journal of Quality Technology* 38(2): 89-104.

WOODALL W.H., ADAMS B.M., & BENNEYAN J.C., 2012, The use of control charts in healthcare, In F. W. Faltin, R. Kenett, and F. Ruggeri (Eds.), *Statistical Methods in Healthcare*, John Wiley & Sons, Inc., pp.253-267.

XIE, M., HE, B., and GOH, T.N., 2001, Zero-inflated Poisson model in statistical process control. *Computational Statistics and Data Analysis* 38(2): 191-201.

LIST OF ABBREVIATIONS AND NOTATIONS

EED	Early event detection
EWMA	Exponentially Weighted Moving Average
S_t	Shewhart statistic
h	Threshold
ZIP	Zero-inflated Poisson
λ	Weighting parameter
c	Determining constant for Shewhart ZIP-based threshold
$\bar{y}^+$	Mean number of all counts greater than zero
Z_t	EWMA statistic
Y_t	Observation at time t
μ_0	Process mean of all in-control observations (without outbreaks)
L	Determining constant for EWMA threshold
ATFS	Average time between false signals
CED	Conditional expected delay
PSD	Probability of successful detection
PTS	Proportion of true signals
PDO	Proportions of detections in an outbreak
t*	Time of first signal inside an outbreak
t**	Time of second signal inside an outbreak
τ_s	Start time period of outbreak
τ_l	Last time period of outbreak
ARL_0	Average run length when the process is in-control
ARL_1	Average run length when the process is out-of-control
τ_r	Last significant time period in the outbreak for detection
$Y_{\tau i}$	Any EED method statistic observed at time τ_i
θ	Expected number of occurrences at time i
π	Probability of additional zeros
o_t	Additive term denoting outbreaks
M	Maximum magnitude of an outbreak
D	Duration of outbreak
τ	Starting time of outbreak within dataset (usually set to 1)
CV	Coefficient of variation